Wearable Motion Tolerant PPG Sensor for Instant Heart Rate in Daily Activity

Takanori Ishikawa[1], Yasuhide Hyodo[1], Ken Miyashita[2], Kazunari Yoshifuji[1], Yota Komoriya[1] and Yutaka Imai[1]

[1]*Interface Device Development Dept., UI Device Development Div., Device & Material R&D Group, R&D Platform, Sony Corporation, 4-14-1 Asahi-cho, 243-0014, Atsugi-shi, Kanagawa, Japan*

[2]*Intelligent Application Technology Development Dept., Application Technology Development Div., System R&D Group, R&D Platform, Sony Corporation, 2-10-1 Osaki, 141-8610, Shinagawa-ku, Tokyo, Japan*

Keywords: PPG Sensor, Motion Artifact Cancellation Framework, Heart Rate Variability, Daily Activity, Ambulatory.

Abstract: A wristband-type PPG heart rate sensor capable of overcoming motion artifacts in daily activity and detecting heart rate variability has been developed together with a motion artifact cancellation framework. In this work, a motion artifact model in daily life was derived and motion artifacts caused by activity of arm, finger, and wrist were cancelled significantly. Highly reliable instant heart rate detection with high noise-resistance was achieved from noise-reduced pulse signals based on peak-detection and autocorrelation methods. The wristband-type PPG heart rate sensor with our motion artifact cancellation framework was compared with ECG instant heart rate measurement in both laboratory and office environments. In a laboratory environment, mean reliability (percentage of time within 10% error relative to ECG instant heart rate) was 86.5% and the one-day pulse-accuracy achievement rate based on time use data of body motions in daily life was 88.1% or approximately 21 hours. Our device and motion artifact cancellation framework enable continuous heart rate variability monitoring in daily life and could be applied to heart rate variability analysis and emotion recognition.

1 INTRODUCTION

A variety of applications using wristband-type, photoplethysmography (PPG)-based heart rate sensors have been proposed in recent years. Their typical applications are heart rate monitoring in a resting state for healthcare, feedback to efficient training methods in walking and running state as well as estimation of consumed calories. These applications are based on averaged heart rate to reduce motion artifact.

Though accurate monitoring of heart rate variability (HRV) has not yet been achieved in motion state, once it is achieved, it will open a variety of applications including like music recommendation based on user affective state, stress monitoring and cardiac insufficiency detection (Wijsman, 2013); (Shin, 2014); (Venema, 2015).

In comparison with chest-strap-type wearable electrocardiography (ECG) monitors, wristband-type PPG heart rate sensors can be comfortably worn without placing a burden on the user, which gives them a user-friendly advantage. On the other hand, wristband-type PPG sensors suffer from a superimposing of pseudo pulse signals (motion artifacts) caused by user motion, which makes accurate calculation of heart rate difficult (Tamura, 2014). Consequently, to accurately calculate pulse rate from pulse signals superimposed with motion artifacts, various types of motion artifact reduction methods have been proposed to improve accuracy of HRV from PPG raw data(Renevey, 2001); (Asada, 2004), and there have been many studies targeting periodic motion artifacts caused by intense arm motion while walking or running. So far many studies have reported evaluation average pulse rate using average heart rate by ECG as reference.

Focusing on motion in daily life, we have to take into account random motion of arm, finger and wrist. An experimental protocol was proposed that includes activity of both arm, finger and wrist (Parak, 2014); (Binsch, 2016); (Tăuţan, 2015), but their study was limited to evaluation and analysis of motion artifact.

Ishikawa T., Hyodo Y., Miyashita K., Yoshifuji K., Komoriya Y. and Imai Y.
Wearable Motion Tolerant PPG Sensor for Instant Heart Rate in Daily Activity.
DOI: 10.5220/0006109901260133
In *Proceedings of the 10th International Joint Conference on Biomedical Engineering Systems and Technologies (BIOSTEC 2017)*, pages 126-133
ISBN: 978-989-758-212-7

In this paper, we report on a motion artifact cancellation framework that we have developed based on the results of analyzing arm and finger motion artifacts assuming motions in daily life. We also report on laboratory and ambulatory evaluation of this framework using instant heart rate by ECG as reference with our design of experimental protocols simulating motions in daily life.

2 PROBLEM STATEMENT

2.1 Photoplethysmography

The reflective PPG method measures changes in blood flow in subcutaneously distributed capillaries by injecting light from a light source into the skin and measuring the intensity of returning light by a receiver after absorption and diffusion by blood flow and skin tissue several mm under the skin (Renevey, 2001).

$$I_o(t) = I_i \cdot \gamma_{pulse}(t) \cdot \gamma_{tissue} \quad (1)$$

Here, I_i is the intensity of the light incident on the skin, $\gamma_{pulse}(t)$ is the temporal change in diffusion and absorption by hemoglobin, etc. in capillary blood flow, γ_{tissue} is the amount of diffusion and absorption by body tissue, and $I_o(t)$ is the intensity of reflected light.

2.2 Motion Artifact

There are activities of arm, finger and wrist in daily life affecting wristband-type PPG sensors. In the case of finger and wrist motions, the muscles under the wrist move causing the state of blood flow in subcutaneous body tissue to change. This would mean that γ_{tissue} in Eq. (1) is not fixed. We therefore performed an analysis of motion artifacts caused by arm and finger motion in the following way.

While the thickness of each layer under the skin differs by site, age, etc., body tissue lies at a depth of 1.0 – 2.0 mm (Boucsein, 2012). To measure the state of blood flow in subcutaneous tissue in a non-invasive manner, we adopted the PPG method. Taking into account the subcutaneous penetration of light (Bashkatov, 2005) and the optical absorption and diffusion coefficients of hemoglobin, we determined an optimal wavelength as follows. First, we analyzed the optical wavelength dependency of the signal-to-noise ratio (S/N) by measuring the pulse signal when bending and stretching the index finger periodically (2 Hz) and performing a frequency analysis. In calculating S/N, we took the heart-rate band as the signal band and defined the finger-motion frequency band as the noise band.

Table 1: LED wavelength dependency of S/N when bending and stretching the index finger periodically.

Subject	470nm	530nm	630nm	860nm	940nm
#1	1.90	7.75	-7.22	-5.66	-5.75
#2	2.25	7.61	-18.30	-10.20	-15.47
#3	7.72	4.67	-13.02	-7.95	2.83

Table 1 lists the wavelength dependency of S/N when bending and stretching the index finger periodically as measured with three subjects. The wavelengths used in this analysis are those of easily obtainable LEDs. These results show that S/N is smallest for a wavelength of 630 nm, so we chose it to be the optical wavelength of the PPG signal that reflects finger motion well.

However, for the pulse signal, we chose a wavelength of 530 nm to measure the state of blood flow in the capillaries of the dermic layer that is not easily affected by body tissue (Faber, 2004); (Lee, 2013). Here, we simultaneously measured the arm's acceleration signal by having a 3-axis acceleration sensor worn on the wrist.

Figure 2 (A) shows the results of a PPG (green) and acceleration frequency analysis when moving the arm back and forth with a 2 Hz period in a standing position. Strong peaks are observed in the PPG (green) spectral distribution near the arm-moving frequency of 120 [bpm] and the heartbeat frequency of 100 [bpm]. This shows that the arm-related motion artifact is superimposed as a pseudo pulse signal. Since a motion artifact is easily superimposed when blood is flowing, it is thought that body motion affects blood flow and a pseudo pulse signal arises due to pseudo blood flow.

Figure 2 (B) shows the results of a PPG (green) and a PPG (red) frequency analysis when bending and stretching the index finger periodically at 1.5 Hz while keeping the arm fixed in a sitting position. Although the acceleration sensor measured no finger motion, a strong peak is observed near the finger-moving frequency of 90 [bpm] in the PPG (green) and PPG (red) spectral distributions. In particular, the PPG (red) spectral distribution shows that the spectral intensity at the motion artifact frequency of 90 [bpm] is stronger than that at the heartbeat frequency of 60 [bpm] compared with PPG (green). This is thought to be that the hemoglobin diffusion coefficient is smaller and the degree of subcutaneous penetration deeper at 630 nm than at 530 nm. Therefore, we suppose that intensity of returning

light from skin is smaller compares with wavelength of 530nm. Furthermore, we have observed that motion artifact caused by wrist motion has same characteristic in frequency analysis.

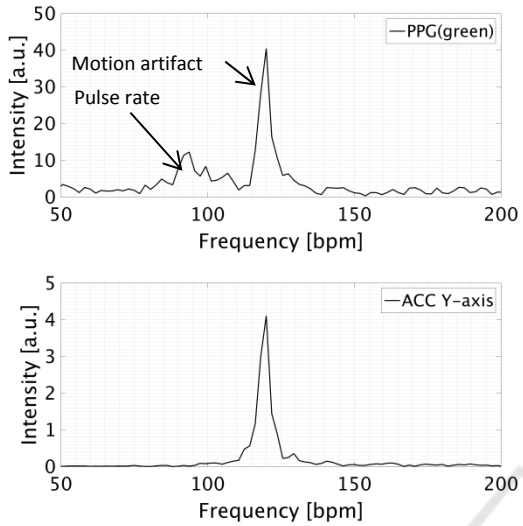

(A) When moving the arm back and forth at 2 Hz

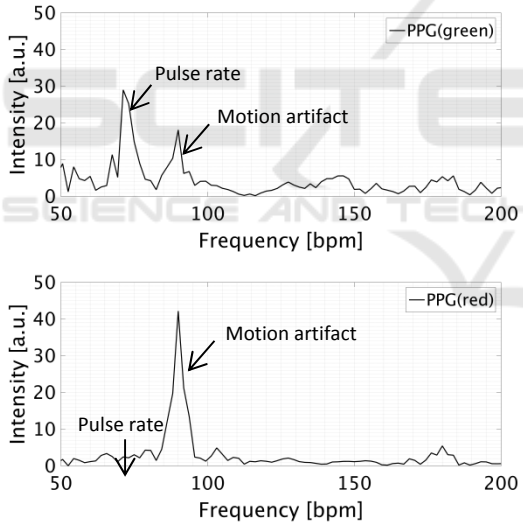

(B) When bending and stretching the index finger at 1.5 Hz

Figure 2: Results of frequency analysis. (A) upper: PPG (green), lower: acceleration signal (Y-axis means fingertip direction); (B) upper: PPG (green), lower: PPG (red).

Figure 3 shows the results of measuring PPG (green) and acceleration signal in the fingertip direction when moving the arm up and down relative to the heart in a standing position. When the arm is moved above the heart, the total amount of blood flow decreases due to the effect of gravity. Therefore, baseline of the intensity of return light decreases.

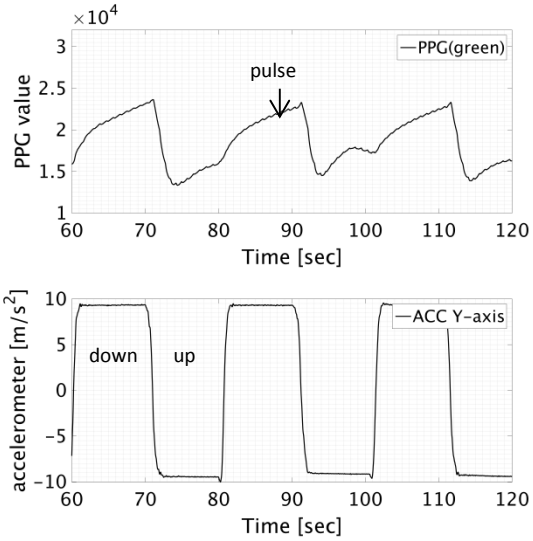

Figure 3: Up-and-down arm motion relative to heart. Upper: PPG (green), lower: acceleration signal.

Conversely, when moving the arm below the heart, it can be seen that this baseline increases. Since the baseline stabilizes in approximately two seconds after lifting the arm, noise frequency is assumed to be under 0.5 Hz. The above experimental results show that the intensity of return light from skin is affected by activity of arm, finger and wrist. We can therefore extend Eq. (1) as follows.

$$I_o(t) = I_i \cdot \gamma_{pulse}(t) \cdot \gamma_{tissue}(t) \cdot \gamma_{motion}(t) \cdot \gamma_{gravity}(t) \quad (2)$$

Here, $\gamma_{tissue}(t)$ is the amount of optical absorption and diffusion in body tissue due to finger motion, $\gamma_{motion}(t)$ is the amount of optical absorption and diffusion due to changes in blood flow caused by arm motion, and $\gamma_{gravity}(t)$ is the amount of optical absorption and diffusion due to the arm's up or down orientation. If we now take the logarithm of both sides of this equation, Eq. (2) can be rewritten as follows.

$$y(t) = s(t) + n_t(t) + n_m(t) + n_g(t) \quad (3)$$

Here, $s(t)$ is the pulse signal, $n_t(t)$ is the noise signal due to finger motion, $n_m(t)$ is the noise signal due to arm motion, and $n_g(t)$ is the noise signal due to arm orientation. In other words, this equation shows that all motion artifacts in the PPG method are superimposed on the observed signal.

3 PROPOSED METHOD

A motion artifact cancellation framework based on Eq. (3) that assumes an additive model for arm and finger motion artifacts is shown in Figure 4.

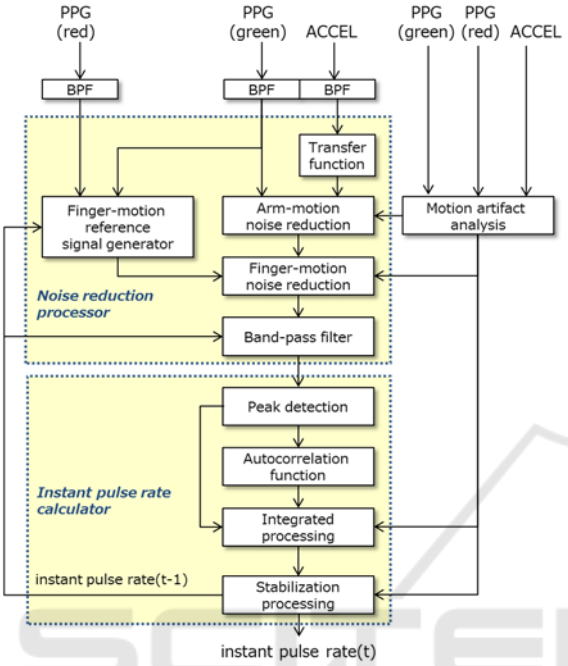

Figure 4: Schematic diagram of motion artifact cancellation framework.

To first step in this framework is to separate the motion artifact due to the orientation of the arm using a band-pass filter (BPF). Here, the pass band is set to [0.5, 5] Hz taking into account the arm-orientation noise band and the heart-rate frequency band.

The next step is to separate arm-motion noise by an adaptive filter using the acceleration signal as a reference signal. It is important in noise reduction processing using an adaptive filter to select a reference signal having high correlation with the noise signal superimposed on the observed signal (Asada, 2004). For this reason, we modelled beforehand the transfer function to body-motion blood flow as a finite impulse response (FIR) filter through system identification. The signal resulting from the convolution of the acceleration signal with the FIR filter is used as a reference signal for arm-motion noise reduction processing.

Similarly, finger-motion noise is separated using a reference signal. Here, we use the PPG signal as a reference signal to make non-invasive measurements of the state of blood flow in body tissue. We decided that an optical wavelength is 630 nm based on previous analysis results in Table 1.

However, a pulse signal component is also included in PPG (red). To therefore make correlation with the noise signal even higher, we use a BPF to weaken the pulse signal component based on the finally estimated heart rate. Furthermore, assuming use in ambulatory environment and knowing that noise will also be generated by changes in contact pressure caused by deformation of the arm's shape, we also use a BPF to reduce this noise.

Next is the calculation of the instant pulse rate from the pulse signal reduced of motion artifacts. Although peak detection is applied here to calculate the instant pulse rate, erroneous detections can easily occur due to the effects of residual noise. To deal with this noise, we introduce pulse rate detection by an autocorrelation function exploiting the periodicity of the pulse signal. Pulse rate calculation by an autocorrelation function calculates the inter-beat-interval (IBI) from the lag at which the correlation function becomes maximum. However, while the autocorrelation method is highly robust to noise, its assumption of periodicity in the pulse signal can result in lower accuracy than the peak detection method if pulse variability are present. For this reason, the integrated processing section in this framework first calculates the instant pulse rate by both the peak detection method and autocorrelation method and the reliability of each result. It then outputs the optimal instant pulse rate based on the pulse signal and body motion information analyzed from the acceleration signal.

4 EXPERIMENTAL VALIDATION

4.1 Heart Rate Sensor Prototype

Our prototype for a wristband PPG heart rate sensor is shown in Figure 5. This device performs pulse signal measurement by irradiating the human body with green LED light and measuring reflected light with a photodetector. It also performs reference-signal measurement in the finger-motion noise-reduction process by measuring reflected light from a red LED likewise with a photodetector. In addition, it obtains a reference signal in the arm-motion noise-reduction process by measuring arm acceleration with a 3-axis acceleration sensor built into the sensor enclosure. The pulse signal obtained from measured green-LED and red-LED light and the acceleration signal are recorded in built-in eMMC flash storage. The sampling frequency is 128 Hz for all sensors.

The device incorporates a real-time clock (RTC) that can be synchronized with a host PC and recorded together with measured data.

Figure 5: Prototype of wristband type heart rate sensor.

4.2 Subjects

The experiment was conducted with 12 subjects recruited from male employees in the workplace. After obtaining approval from the Sony Life Ethics Committee, the subjects were briefed about the contents of this research project and their consent was obtained in writing.

Table 2: Subjects.

Characteristic	$\mu \pm \sigma$	Range
Age	35.00 ± 6.34	26 – 43

4.3 Laboratory Protocol and Evaluation

Evaluating motion artifacts in daily life requires knowledge of user lifestyle for users wearing a wristband-type device. Although there are various types of user lifestyles, activity time use by types of behavior for one week can be summarized as follows according to material from the Statistics Bureau of the Ministry of Internal Affairs and Communications (MIC) (Ministry of Internal Affairs and Communications, 2011). However, an evaluation based on protocol that mimics these activities as-is puts an unrealistic burden on subjects, so we designed original protocols after reclassifying activities into three main states of body motion.
These are (1) active state featuring periodic arm motion of fixed intensity as in walking when commuting to school or work or engaging in sports (such as jogging or running), (2) semi-resting state featuring non-periodic arm motion of random intensity and finger activity as in schoolwork, work, housework, meals, etc. and (3) resting state as in sleeping. The results of reorganizing the above activities are listed on Table 4.

Table 3: Detailed activity time use by types of behavior for one week.

Activity	Duration (hh:mm)
Sleep	07:42
Personal care	01:19
Meals	01:39
Commuting to and from school or work	00:31
Work	03:33
Schoolwork	00:39
Housework	01:27
Caring or nursing	00:03
Child care	00:14
Shopping	00:26
Moving (excluding commuting)	00:30
Watching TV, listening to the radio, reading a newspaper or magazine	02:27
Rest and relaxation	01:31
Learning, self-education, and training	00:12
Hobbies and amusements	00:44
Sports	00:14
Volunteer and social activities	00:04
Social life	00:19
Medical examination or treatment	00:08
Other activities	00:17

Table 4: Results of reclassifying activity time use by types of behavior.

Class	Duration (%)
Resting state	32.8
Semi-resting state	65.1
Active state	3.1

Specifically, we designed three types of protocols based on the above results of reclassifying activity time use by types of behavior. First, to evaluate periodic motion artifacts in an active state, we designed a “run” protocol which is taken into account for walking when commuting to school or work or engaging in sports such as jogging or running. Next, to evaluate non-periodic motion artifacts in a semi-resting state, we designed “daily1” and “daily2” protocols which are taken account for habitual tasks in daily life and business-related work, schoolwork, housework, etc. For each protocol, the subject began by resting in a sitting position to condition his heart rate. All three protocols were not performed on the same day to lighten the load on subjects.

We used the Shimmer3 ECG unit from Shimmer to provide a reference measurement for instant heart rate. The sampling frequency is 512 Hz. Electrode positioning was also optimized for each subject to enhance S/N of the ECG signal. The instant heart rate was calculated from the time intervals of the R

Table 5: Run protocol.

Task	Duration (min)
Take deep breaths sitting down	2
Stand and rest	1
Walk on treadmill at 5 km/h	3
Walk on treadmill at 7 km/h	3
Walk on treadmill at 11 km/h	3
Take a break standing up	2

Table 6: Daily1 protocol.

Task	Duration (min)
Take a break sitting down	2
Take deep breaths sitting down	2
Gesture that is supposed personal care	2
Gesture that is supposed meals	2
PC operation that is supposed office work	2
Smart phone operation	2
Gesture that is supposed housework	2
Take a break sitting down	2

Table 7: Daily2 protocol.

Task	Duration (min)
Take a break sitting down	2
Gesture that is supposed reading book	2
Gesture that is supposed writing down	2
Gesture that is supposed conversation	2
Take a break sitting down	2

wave in the ECG signal.

The subject wore the prototype PPG sensor on his non-dominant hand, and time synchronization with shimmer3 was achieved through time synchronization between the prototype device and the host PC.

In comparing the instant heart rate calculated from ECG and the instant pulse rate calculated from the prototype device, we used resampled values at 1 Hz by linear interpolation for each. Furthermore, in performing a quantitative evaluation of the accuracy of detecting heart rate variability, we defined reliability and accuracy as follows (Delgado-Gonzalo, 2014).

Reliability is defined as the percentage number of samples for which error is within 10% of the ECG instant heart rate. Accuracy, meanwhile, is the mean complement of error with the ECG instant heart rate.

Table 8 lists mean reliability and accuracy across all subjects for each protocol in a laboratory environment. Figure 6 shows Bland-Altman plots of the ECG instant heart rate and PPG instant pulse rate for each experimental protocol.

Table 8: Subject mean of reliability and accuracy of estimated instant heart rate for each protocol in a laboratory environment (*Accuracy = 100 - mean percentage error).

Protocol	Reliability (%)	*Accuracy (%)
Run protocol	83.7	93.9
Daily1 protocol	82.7	93.8
Daily2 protocol	93.0	96.1
Mean	86.5	94.6

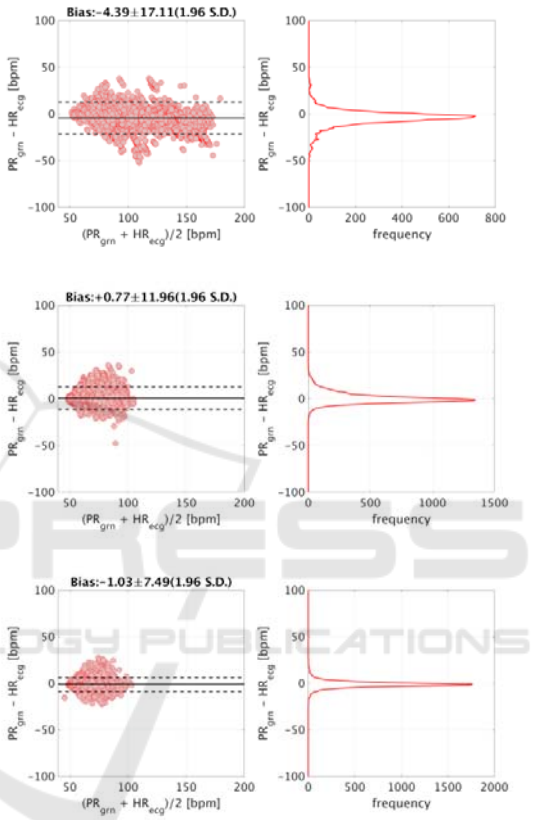

Figure 6: Results of Bland-Altman analysis of ECG instant heart rate and PPG instant pulse rate. Top: run protocol; middle: daily1 protocol; bottom: daily2 protocol. HR_{ecg} and PR_{grn} denote ECG instant heart rate and PPG instant pulse rate, respectively.

Based on the quantitative evaluation results for each experimental protocol of Table 8 and activity time use by types of behavior of Table 4, we estimated the percentage of measurements within 10% of the ECG heart rate for one day (referred to below as "pulse-accuracy achievement rate") in the following way. Reliability of resting state was taken to be reliability in a resting state over the run protocol, daily1 protocol, and daily2 protocol. As a result, subject mean of them was 97.5%. Next, reliability of active state was taken to be reliability in the range

from standing to running tabulated for the run protocol. As a result, subject mean of reliability was 81.4%. Finally, reliability of semi-resting state was taken to be reliability outside the resting state tabulated over the daily1 protocol and daily2 protocol. As a result, subject mean of them was 83.7%. Based on the above results, the day pulse-accuracy achievement rate turned out to be 88.1% or 21.1 hours when converted to time.

5 DISCUSSION

We evaluated the reliability and accuracy of the prototype wristband-type PPG sensor and motion artifact cancellation framework in ambulatory environment. In the experiment, we randomly selected 4 of the 12 subjects and took pulse measurements during their working hours. Table 9 lists reliability and accuracy values for each of these subjects. Body motions from the subjects' activity records were typically computer keyboard operations, note-taking/writing, lunch, and smartphone use during breaks, which means activities near those of the daily1 and daily2 protocols. However, reliability in an office environment was found to be 77.9% or about 10% lower than the 87.9% average reliability of the daily1 and daily2 protocols.

Table 9: Subject mean of reliability and accuracy of instant heart rate estimation in an office environment.

Subject	Duration (hh:mm)	Reliability (%)	Accuracy (%)
#1	08:00	68.7	91.4
#2	08:00	84.1	94.3
#3	08:00	77.9	93.3
#4	08:00	80.9	93.8
Mean (N=4)	08:00	77.9	93.2

Figure 7 shows Bland-Altman plots of the ECG instant heart rate and PPG instant pulse rate. Compared with the Bland-Altman plots for the daily1 and daily2 protocols of Figure 6, the heart rate band has broadened and estimation error of the instant heart rate has increased. This broadening of the heart rate band can be explained as follows. For the daily1 and daily2 protocols in a laboratory environment, subjects carried out their tasks in a sitting position, but in the office-environment experiment, their heart rates would increase as they walked to conference rooms or cafeterias or engaged in discussions during meetings. Next, the increase in error is thought to be due to changes in contact pressure between the pulse sensor and subject's body due to deformation of the arm's shape caused by motion or twisting of the wrist. If motion artifacts due to changes in contact pressure can be formalized as an additive model, our proposed framework should be able to incorporate them.

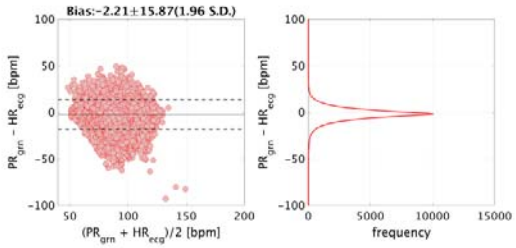

Figure 7: Results of Bland-Altman analysis of ECG instant heart rate and PPG instant pulse rate in an office environment. HR_{ecg} and PR_{grn} denote ECG instant heart rate and PPG instant pulse rate, respectively.

6 CONCLUSIONS

We proposed a motion artifact cancellation framework for a wristband-type heart rate sensor. As part of this framework, we derived a motion artifact additive model based on the results of motion artifact analysis.

First, to cancel arm-related motion artifacts, we modelled the transfer function to blood flow as an FIR filter through system identification and used the signal resulting from convolution of the acceleration signal as a reference signal to improve the arm-related motion artifact reduction effect. Next, to cancel finger and wrist-related motion artifacts, we measured blood flow in body tissue by PPG at 630 nm, weakened the pulse-signal component in that signal by a band-pass filter based on heart rate, and used the result as a reference signal to improve the finger-related motion artifact reduction effect.

Finally, for pulse rate calculation, we integrated the results of calculating pulse rate with reliability by both the peak-detection and autocorrelation methods thereby achieving instant pulse rate detection with high noise resistance and high accuracy. The pulse-measurement accuracy-achievement rate was estimated to be 88.1% or 21.1 hours, which indicates that the prototype device and motion artifact cancellation framework can detect variability in heart rate with high accuracy in daily activity.

REFERENCES

Wijsman, J., Vullers, R., Polito, S., Agell, C., Penders, J., Hermens, H., 2013. Towards Ambulatory Mental Stress Measurement from Physiological Parameters. In *Affective Computing and Intelligent Interaction*, pp. 564 - 569.

Shin, I. H., Cha, J., Cheon, G. W., Lee. C., Lee, S. Y., Yoon, H. J., Kim, H. C., 2014. Automatic stress-relieving music recommendation system based on photoplethysmography-derived heart rate variability analysis. In *36th Annual International Conference of the IEEE Engineering in Medicine and Biology Society*, pp. 6402-6405.

Venema, B., Blazek, V., Leonhardt, S., 2015. In-Ear Photoplethysmography for Mobile Cardiorespiratory Monitoring and Alarming. In IEEE 12th International Conference on Wearable and Implantable Body Sensor Networks, pp. 1-5.

Tamura, T., Maeda, Y., Sekine M. and Yoshida M., 2014. Wearable Photoplethysmographic Sensors—Past and Present. In *Electronics*, vol. 3, pp. 282-302.

Renevey, P., Vetter, R., Krauss, J., Celka, P., Depeursinge, Y., 2001. Wrist-located pulse detection using IR signals, activity and nonlinear artifact cancellation. In *Engineering in Medicine and Biology Society, Proceedings of the 23rd Annual International Conference of the IEEE*, vol. 3, pp. 3030-3033.

Asada, H. H., Jiang, H. H., Gibbs, P., 2004. Active noise cancellation using MEMS accelerometers for motion-tolerant wearable bio-sensors. In *Engineering in Medicine and Biology Society, 26th Annual International Conference of the IEEE*, vol. 1, pp. 2157-2160.

Parak, J., Korhonen, I., 2014. Evaluation of wearable consumer heart rate monitors based on photopletysmography. In *36th Annual International Conference of the IEEE Engineering in Medicine and Biology Society*, pp. 3670-3673.

Binsch, O., Wabeke, T., Valk, P., 2016. Comparison of three different physiological wristband sensor systems and their applicability for resilience- and work load monitoring. In *13th International Conference on Wearable and Implantable Body Sensor Networks*, pp. 272-276.

Tăuţan, A. M., Young, A., Wentink, E., Wieringa, F., 2015. Characterization and reduction of motion artifacts in photoplethysmographic signals from a wrist-worn device. In *37th Annual International Conference of the IEEE Engineering in Medicine and Biology Society*, pp. 6146-6149.

Ministry of Internal Affairs and Communications, Statistics Bureau, 2011. Basic survey on social life. http://www.stat.go.jp/data/shakai/2011/pdf/gaiyou2.pdf.

Boucseinm W., 2012. *Electrodermal Activity*, Springer. 2nd edtion.

Bashkatov, A. N., Genina, E. A., Kochubey, V. I. and Tuchin, V. V., 2005. Optical properties of human skin, subcutaneous and mucous tissues in the wavelength range from 400 to 2000 nm. In *Applied Physics*, vol. 38, number 15.

Faber, D. J., Aalders, M. C. G., Mik, E. G., Hooper, B. A., Gemert, M. J. C., Leeuwen, T. G., 2004. Oxygen Saturation-Dependent Absorption and Scattering of Blood. In *PHYSICAL REVIEW LETTERS*, vol. 93, number 2.

Lee, J., Matsumura, K., Yamakoshi, K., Rolfe, P., Tanaka, S., Yamakoshi, T., 2013. Comparison between red, green and blue light reflection photoplethysmography for heart rate monitoring during motion. In *35th Annual International Conference of the IEEE Engineering in Medicine and Biology Society*, pp. 1724-1727.

Delgado-Gonzalo, R., Parak, J., Tarniceriu, A., Renevey, P., Bertschi, M., Korhonen, I., 2014. Evaluation of accuracy and reliability of PulseOn optical heart rate monitoring device. In *37th Annual International Conference of the IEEE Engineering in Medicine and Biology Society*, pp. 430-433.